Archives of Mechanics • Archiwum Mechaniki Stosowanej • 27, 3, pp. 385–406, Warszawa 1975

Combined dynamic loading on elastic/viscoplastic tube

J. BEJDA (WARSZAWA) and H. FUKUOKA (TOYONAKA)

The problem of stress wave propagation in an elastic viscoplastic tube under combined axial and torsional impact is examined. To describe dynamic behaviour of material, PERZYNA's constitutive equations were applied. The system of governing equations was solved numerically by the method of finite differences along characteristics. The main features of the solution for mild steel and aluminum are presented in the form of several diagrams. The analysis of propagation velocities of longitudinal and shear loading and unloading waves and the attenuation of their amplitudes are disscussed in detail.

Rozważany jest problem propagacji fal naprężenia w cienkościennej sprężysto lepkoplastycznej rurze pod wpływem jednocześnie przyłożonego, nagłego, osiowego i skrętnego obciążenia. Do opisu dynamicznego zachowania się materiału przyjęto równania konstytutywne PERZYNY. Podstawowy układ równań rozwiązano numerycznie metodą różnic skończonych wzdłuż charakterystyk. Główne wyniki rozwiązania przedstawione zostały w postaci licznych wykresów. Przeprowadzono szczegółową dyskusję prędkości propagacji podłużnych i poprzecznych fal obciążenia i odciążenia oraz ich tłumienia.

Исследуется задача о распространении волн напряжений в упруго-вязкопластической трубе при одновременных осевом и крутительном ударах. Для описания динамического состояния материала принимается определяющие уравнения Пежины. Основную систему уравнений решено численным методом конечных разностей вдоль характеристик. Главные результаты решения представлены в виде нескольких графиков. Подробно обсуждаются скорости распространения продольных и поперечных волн нагрузки и разгрузки, а также их затухание.

1. Introduction

FURTHER theoretical investigations of plastic wave propagation phenomenon are necessary to complement the experimental examinations. Nowadays there are two ways to study experimentally the mechanical behaviour of material under dynamic loading:

1) to obtain the constitutive equations of material using short specimen which is assumed to be uniformly deformed;

2) to observe the wave propagation phenomenon in a long specimen.

The second way of experiments, in particular concerned with the propagation of incremental pulses in thin-walled tubes plastically loaded by combined tension-torsion loads, is of special interest. Such a test for stress state beyond the elastic limit of the material is expected to provide useful information regarding the dynamic plastic behaviour of solids under combined stress states and this information is of fundamental importance in the development of a three-dimensional theory of plastic wave propagation. Besides, this is the only possible way to perform the experiments in combined state of stress comparatively easily.

A theory for wave propagation phenomena in a thin-walled tube based on rate-independent plasticity was first examined by CLIFTON [1] and FUKUOKA [2]. The stress and

strain paths for combined longitudinal and torsional impact loading of a semi-infinite tube initially prestressed to the plastic range by combined static longitudinal and torsional loads were obtained in [1]. It was found that there are three types of stress path according to the value of combined step loading and that in particular there is a region which cannot be reached without unloading in spite of the loading side.

Experiments verifying this theory were performed by LIPKIN and CLIFTON [3] and by FUKUOKA and MASUI [4].

In the apparatus designed by FUKUOKA and MASUI [4], the tube is prestressed quasi-statically to the arbitrary values of tensile and shear stresses and then the incremental impact loadings are superposed. Measurements are made of strain-time profiles at some stations along the tube. A comparison of theoretical and experimental results, made in [5], leads to the following main conclusions. In the case of longitudinal impact, the strain response at the gages qualitatively corresponds to the arrival of a fast wave for which torsional strain decreases, while longitudinal strain increases followed by a slow simple wave for which both torsional and longitudinal strains increase. But in the case of torsional impact, the strain response does not correspond to the theoretical results. In all cases the velocity of propagation of wave front was found to be that of the elastic one.

Theory of combined plastic waves in a thin-walled tube was further widely developed in a series of papers by TING [6, 7, 8]. In [7] he has given a unified treatment of all known in literature combined plastic stress wave problems including both kinematic and isotropic work-hardening of material considered by GOEL and MALVERN [9], and also other problems which have not yet been studied in detail.

Almost none experiments were done for the propagation of combined plastic waves in strain-rate sensitive materials. To compare the experimental and theoretical results, first a corresponding theory for strain rate-dependent material is needed to predict the main features of the wave propagation phenomenon. Thus the aim of this paper is the thorough numerical examination of the stress wave propagation process in an elastic viscoplastic tube under combined impact of longitudinal and torsional load. The combined waves propagating in a strain rate-dependent materials were first studied theoretically for a particular case of plane shear-pressure elastic viscoplastic waves by S. KALISKI and others [10–12]. The compilation of a large number of results concerning the problem of combined waves propagation in a rate-dependent plastic materials is given in [13]. However, until recent time, except short note [14], there appears to be no detailed analysis of incremental wave propagation phenomenon in a prestressed elastic-viscoplastic tube(1). Such analysis is presented in this paper. Special emphasis is laid on the proper choice of constitutive equations describing dynamic behaviour of rate-dependent plastic materials. In our opinion, PERZYNA's constitutive equations [15] are the only well elaborated and widely discussed constitutive equations, and therefore were applied in our investigation. The material constants and the shape of the relaxation function for mild steel and aluminium were chosen on the basis of one-dimensional experimental data. The system of

(1) During preparation of this paper has appeared an interesting work by CLIFTON and HSU [16] which contains an analysis of the propagation of plastic waves in a rate-sensitive plastic materials. Both experimental and theoretical results of combined stress waves in a thin-walled tube are presented. As a rate-dependent plastic material the authors consider commercially pure alpha-titanium (Ti-50A).

governing equations was solved numerically by the method of finite differences along characteristics. In the analysis of the convergence and stability of the difference solution, the emphasis is made on the energy method. The main features of the solution are given in the form of several diagrams. The analysis of velocities of longitudinal and shear loading and unloading waves and the attenuation of their amplitudes are discussed in detail. Attention is also paid to the distribution of the stress gradients with the propagation of front of the wave.

2. Governing equations

Consider a long slender thin-walled cylindrical tube of the mean radius R as shown in Fig. 1. The theory considered is one-dimensional, the material is homogeneous and isotropic, elastic and plastic strain rates are separable, strains are assumed to be small

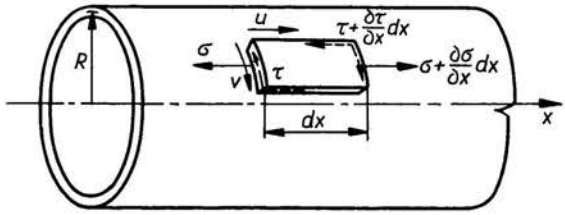

FIG. 1. Stresses and velocities in the tube.

and radial inertia effects are neglected. Under these assumptions and neglecting the change in the mean radius R the non-zero stress components are

$$\sigma_{xx}(x,t) = \sigma, \quad \tau_{x\theta}(x,t) = \tau_{\theta x}(x,t) = \tau \tag{2.1}$$

and the velocity components in axial and circumferential direction are respectively

$$u(x,t) = u, \quad v(x,t) = v. \tag{2.2}$$

Conservation of linear and angular momentum gives

$$\varrho u_t = \sigma_x, \quad \varrho v_t = \tau_x, \tag{2.3}$$

where ϱ is the mass density and suffixes t and x denote partial differentiation with respect to time and spatial coordinate, respectively.

The following compatibility equations hold

$$u_x = \varepsilon_t, \quad v_x = \gamma_t, \tag{2.4}$$

where ε and γ denote longitudinal strain and shearing strain, correspondingly.

To complete the system of governing equations it remains to specify the constitutive equations. The choice of the proper constitutive equations for the dynamic response of rate-dependent plastic material is essential in our analysis. From experimental data it is well known that all real materials are strain rate sensitive. The viscous effects are observed in elastic as well as in plastic range of deformation. A theory describing these effects is complex; difficulties arise specially in proper formulation of the yield criterion in visco-

elastic range of strain. However, following [15] it is sometimes very useful to make certain idealization of the constitutive equations. Assuming that up to the yield point material behaves elastically and viscous effects prevail in a plastic range, we are able to determine in a unique way the yield criterion. In our case it does not differ from the yield criterion well known in classical theory of plasticity. It is thus assumed that the yield function is of the form

$$F(\sigma_{ij}, \varepsilon^p_{ij}) = \frac{f(\sigma_{ij}, \varepsilon^p_{ij})}{\varkappa} - 1, \tag{2.5}$$

where $f(\sigma_{ij}, \varepsilon^p_{ij})$ depends on the stress state σ_{ij} and plastic strain tensor ε^p_{ij}. As we previously assumed, the strain-rate tensor decomposes into elastic and nonelastic parts, i.e. $\varepsilon_{ij} = \varepsilon^e_{ij} + \varepsilon^p_{ij}$, where ε^p_{ij} represents the coupling of viscous and plastic effects, $\varkappa$ is a work-hardening parameter defined as

$$\varkappa = \varkappa(W^p) = \varkappa\left(\int_0^t \sigma_{kl} d\varepsilon^p_{kl}\right), \tag{2.6}$$

where W^p denotes the energy of plastic deformation. There is no unique way of defining the parameter $\varkappa$. The more complicated forms of the work-hardening parameter describing isotropic as well as anisotropic work-hardening of the material, as for example discussed in [17], may be assumed. The yield surface $F = 0$ in nine-dimensional stress-space is assumed to be regular and convex. Under the above assumptions the constitutive equations for strain-rate sensitive plastic materials, proposed first by PERZYNA [18], may be written in a form relating the stress-rate tensor $\dot{\sigma}_{ij}$, strain-rate tensor $\dot{\varepsilon}_{ij}$ and stress tensor σ_{ij}:

$$\begin{aligned} \dot{e}_{ij} &= \frac{1}{2\mu}\dot{s}_{ij} + 2k\gamma_0 \Phi(F)\frac{\partial F}{\partial \sigma_{ij}}, \quad \text{for} \quad F \geqslant 0, \\ \dot{e}_{ij} &= \frac{1}{2\mu}\dot{s}_{ij}, \qquad\qquad\qquad\quad \text{for} \quad F < 0, \\ \dot{\varepsilon}_{kk} &= \frac{1}{3K}\dot{\sigma}_{kk}. \end{aligned} \tag{2.7}$$

Here $\dot{e}_{ij}$ and $\dot{s}_{ij}$ are the components of the strain-rate and stress-rate deviators, respectively, γ_0, k, K and μ denote viscosity coefficient, yield limit in simple shear, bulk modulus and shear modulus, respectively. The first equation of (2.7) holds in viscoplastic region, the second in elastic region and the compressibility equation in both regions. The above equations say that inelastic strain rate is a function of the state of stress which is a difference between actual state and the state corresponding to the static yield criterion. The function of overstresses determines the inelastic strain rate according to the Maxwell viscosity law.

For metals further simplification of the constitutive equations may be made. Reasonable results are obtained even under assumption of the function F in the form

$$F = \frac{\sqrt{J_2}}{k} - 1, \tag{2.8}$$

where J_2 is the second invariant of the stress deviator. In this case the constitutive equations (2.7) take the following simpler form(2):

$$\dot{e}_{ij} = \frac{1}{2}\dot{s}_{ij} + \frac{\gamma}{2} < \Phi\left[\frac{\sqrt{J_2}}{k} - 1\right] > \frac{s_{ij}}{\sqrt{J_2}} \quad \text{for} \quad F \geqslant 0, \tag{2.9}$$

$$\dot{e}_{ij} = \frac{1}{2}\dot{s}_{ij}, \quad \text{for} \quad F < 0, \tag{2.10}$$

$$\dot{\varepsilon}_{ii} = \frac{1}{3K}\dot{\sigma}_{ii}. \tag{2.11}$$

Although further analysis is practically independent of the complexity of the relaxation function Φ, in numerical computation, however, the simple form of constitutive equations is preferable and therefore we shall use the Eqs. (2.9)–(2.11). These equations have been verified experimentally by LINDHOLM [19, 20] and a very good agreement of experimental data with the results predicted by PERZYNA's theory was confirmed for mild steel as well as for aluminium.

It should also be stressed that the phenomenological equations (2.9)–(2.11) have recently obtained proper physical justification [21]. In particular, the mechanisms responsible for plastic effects and rate sensitivity are discussed in detail.

In our problem

$$\sigma_{ij} = \begin{bmatrix} \sigma & \tau & 0 \\ \tau & 0 & 0 \\ 0 & 0 & 0 \end{bmatrix}, \quad s_{ij} = \begin{bmatrix} \frac{2}{3}\sigma & \tau & 0 \\ \tau & -\frac{1}{3}\sigma & 0 \\ 0 & 0 & -\frac{1}{3}\sigma \end{bmatrix}, \tag{2.12}$$

$$F = \frac{\sqrt{\frac{1}{3}\sigma^2 + \tau^2}}{k} - 1, \quad \dot{\varepsilon}_{kk} = \frac{\dot{\sigma}}{3K}$$

and the constitutive equations (2.9)–(2.11) are now:

$$\dot{\varepsilon}_{11} = u_x = \frac{1}{E}\dot{\sigma} + \frac{2}{3}\frac{\gamma}{\sqrt{J_2}}\sigma\Phi(F), \tag{2.13}$$

$$\dot{\varepsilon}_{12} = \frac{1}{2}v_x = \frac{1}{2\mu}\dot{\tau} + \frac{\gamma}{\sqrt{J_2}}\tau\Phi(F). \tag{2.14}$$

The governing equations (2.3) and (2.4), (2.13) and (2.14) may be written in an abbreviated matrix form

$$\mathbf{A}\mathbf{w}_t + \mathbf{B}\mathbf{w}_x + \mathbf{C} = 0, \tag{2.15}$$

(2) Derived in a different way the constitutive equations in [16] do not differ significantly from the equations considered here.

where

$$W = \begin{bmatrix} u \\ v \\ \sigma \\ \tau \end{bmatrix}, \quad \mathbf{A} = \begin{bmatrix} \varrho & 0 & 0 & 0 \\ 0 & \varrho & 0 & 0 \\ 0 & 0 & \frac{1}{E} & 0 \\ 0 & 0 & 0 & \frac{1}{\mu} \end{bmatrix}, \quad \mathbf{B} = \begin{bmatrix} 0 & 0 & -1 & 0 \\ 0 & 0 & 0 & -1 \\ -1 & 0 & 0 & 0 \\ 0 & -1 & 0 & 0 \end{bmatrix}, \tag{2.16}$$

$$\mathbf{C} = \begin{bmatrix} 0 \\ 0 \\ \frac{2\gamma\sigma}{3\sqrt{J_2}}\Phi(F) \\ \frac{2\gamma\tau}{\sqrt{J_2}}\Phi(F) \end{bmatrix}.$$

In elastic range of deformations we put $\gamma = 0$, thus vector $\mathbf{C} = 0$. For comparison, we shall also need the corresponding equations for rate-independent plasticity. In this case the basic system of equations takes the form [1]

$$\mathbf{A}^*\mathbf{w}_t + \mathbf{B}^*\mathbf{w}_x = 0 \tag{2.17}$$

in which $\mathbf{B}^* = \mathbf{B}$, $\mathbf{C} = 0$ and

$$\mathbf{A}^* = \begin{bmatrix} \varrho & 0 & 0 & 0 \\ 0 & \varrho & 0 & 0 \\ 0 & 0 & \frac{1}{E} + \mu\frac{\sigma^2}{\theta^2} & H\sigma\tau \\ 0 & 0 & H\sigma\tau & \frac{1}{\mu} + H\theta^2\tau^2 \end{bmatrix} \tag{2.18}$$

and the yield condition is assumed in the form

$$f(\sigma, \tau) = \left(\frac{\sigma}{\theta}\right)^2 + \tau^2 = k^2, \tag{2.19}$$

where θ is a constant and for $\theta = \sqrt{3}$ the Eq. (2.20) corresponds to the Huber-Mises yield criterion (distorsion energy) and for $\theta = 2$ to the Tresca condition (maximum shear stress), k denotes as previously the yield limit in pure shear,

$$H = \frac{dW^p/dk}{\theta^2 k^3}; \tag{2.20}$$

W^p is plastic work and is determined here as

$$W^p = \sigma\varepsilon^p + \tau\gamma^p. \tag{2.21}$$

3. Characteristic properties of the governing equations and finite differences

3.1. Characteristics and equations along them

Let us examine first the system of the Eqs. (2.15). The matrices **A** and **B** are symmetric and besides, the matrix **A** is positive definite. Thus the Eqs. (2.15) constitute a standard system of the first-order partial differential equations of hyperbolic type studied extensively elsewhere [22]. To derive the differential equations along characteristics, the eigenvalues and eigenvectors associated with the system of the Eqs. (2.15) should be evaluated. The eigenvalues or the characteristic wave velocities determined as the roots of the determinant

$$||c\mathbf{A}-\mathbf{B}|| = 0 \tag{3.1}$$

are

$$c_1 = \sqrt{\frac{E}{\varrho}}, \quad c_2 = \sqrt{\frac{\mu}{\varrho}}, \quad c_3 = -\sqrt{\frac{E}{\varrho}}, \quad c_4 = -\sqrt{\frac{\mu}{\varrho}},$$

where the indices 1 and 2 stand for longitudinal and shear waves, respectively. The left eigenvectors associated with the system of the Eqs. (2.15) serve to determining of the characteristic conditions and are evaluated from the condition

$$l^T(c\mathbf{A}-\mathbf{B}) = 0, \tag{3.2}$$

where the index T is used to indicate the transpose vector. There are the following four eigenvectors:

$$l^1 = \begin{bmatrix} 1 \\ 0 \\ -\varrho c_1 \\ 0 \end{bmatrix}, \quad l^2 = \begin{bmatrix} 0 \\ 1 \\ 0 \\ -\varrho c_2 \end{bmatrix}, \quad l^3 = \begin{bmatrix} 1 \\ 0 \\ \varrho c_1 \\ 0 \end{bmatrix}, \quad l^4 = \begin{bmatrix} 0 \\ 1 \\ 0 \\ \varrho c_2 \end{bmatrix}. \tag{3.3}$$

Multiplying $l^{k(T)}$ by the Eq. (2.15), we obtain the equation

$$\mathbf{l}^{k(T)}\mathbf{A}\mathbf{w}_t + \mathbf{l}^{k(T)}\mathbf{B}\mathbf{w}_x + \mathbf{l}^{k(T)}\mathbf{C} = 0 \tag{3.4}$$

which, after using the condition

$$l^i(cA_{ij}-B_{ij}) = 0 \tag{3.5}$$

holding along characteristics $dx/dt = c$, leads to

$$\mathbf{l}^{k(T)}\mathbf{A}(\mathbf{w}_t + c_k\mathbf{w}_x) = -\mathbf{l}^{k(T)}\mathbf{C}. \tag{3.6}$$

Since on the characteristics we have

$$\frac{d\mathbf{w}}{dt} = c\mathbf{w}_x + \mathbf{w}_t,$$

we obtain finally

$$\mathbf{l}^{k(T)}\mathbf{A}\frac{d}{dt}\mathbf{w} = -\mathbf{l}^{k(T)}\mathbf{C}. \tag{3.7}$$

Thus, for example, for the first eigenvector we obtain explicitly

$$(3.8)\quad (1,0,-\varrho c_1,0)\begin{bmatrix}\varrho & 0 & 0 & 0\\ 0 & \varrho & 0 & 0\\ 0 & 0 & \frac{1}{E} & 0\\ 0 & 0 & 0 & \frac{1}{\mu}\end{bmatrix}\frac{d}{dt}\begin{bmatrix}u\\ v\\ \sigma\\ \tau\end{bmatrix} = -(1,0,-\varrho c_1,0)\begin{bmatrix}0\\ 0\\ \frac{2}{3}\gamma\frac{\sigma}{\sqrt{J_2}}\Phi(F)\\ 2\gamma\frac{\tau}{\sqrt{J_2}}\Phi(F)\end{bmatrix},$$

or

$$(3.9)\qquad \varrho\frac{du}{dt}-\frac{\varrho c_1}{E}\frac{d\sigma}{dt}=\frac{2}{3}\varrho c_1\gamma\frac{\sigma}{\sqrt{J_2}}\Phi(F).$$

Introducing the eigenvectors (3.3) into the Eq. (3.7), we obtain the required ordinary differential equations along characteristics

$$(3.10)\quad \begin{aligned}
&\frac{d}{dt}\left(u-\frac{c_1}{E}\sigma\right)=\frac{2}{3}c_1\gamma\frac{\sigma}{\sqrt{J_2}}\Phi(F) \quad \text{along} \quad \frac{dx}{dt}=\sqrt{\frac{E}{\varrho}},\\
&\frac{d}{dt}\left(v-\frac{c_2}{\mu}\tau\right)=2c_2\gamma\frac{\tau}{\sqrt{J_2}}\Phi(F) \quad \text{along} \quad \frac{dx}{dt}=\sqrt{\frac{\mu}{\varrho}},\\
&\frac{d}{dt}\left(u+\frac{c_1}{E}\sigma\right)=-\frac{2}{3}c_1\gamma\frac{\sigma}{\sqrt{J_2}}\Phi(F) \quad \text{along} \quad \frac{dx}{dt}=-\sqrt{\frac{E}{\varrho}},\\
&\frac{d}{dt}\left(v+\frac{c_2}{\mu}\tau\right)=-2c_2\gamma\frac{\tau}{\sqrt{J_2}}\Phi(F) \quad \text{along} \quad \frac{dx}{dt}=-\sqrt{\frac{\mu}{\varrho}}.
\end{aligned}$$

3.2. Finite differences

The method of finite differences along characteristics is applied to the solution of the system of the Eqs. (2.15). To obtain sufficiently accurate approximate solution, the second-order difference schemes were introduced. Our method is of the second-order accuracy in the sense that if the solution is known at some time t the error introduced in the next step of time $t+\Delta t$ would be $0(\Delta t^3)$. Before deriving the difference equations the phase plane (x, t) was covered by the rectangular mesh net with mesh sizes Δx, Δt, the characteristic element of which is shown in Fig. 2. The ratio $\Delta x/\Delta t$ is chosen in such a way that

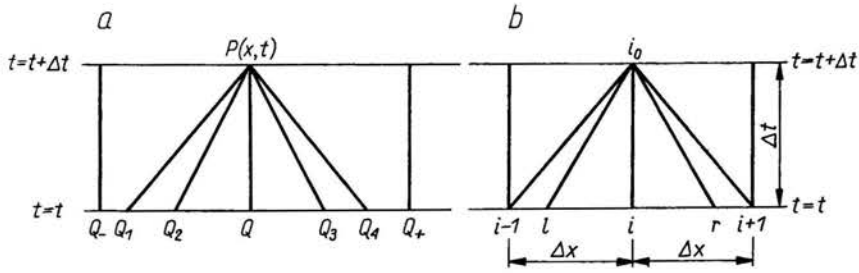

FIG. 2. Elements of the characteristic net for interior points of the phase plane x, t.

the von Neuman stability condition is always satisfied. Taking the ratio $r = \Delta x/\Delta t$ equal to c_1 and denoting for abbreviation

$$D = \frac{\gamma}{\sqrt{J_2}}\Phi(F),$$

the following explicit formulae for the unknowns u, v, σ, τ in the inner points P_i^0 (Fig. 2) are obtained:

$$\begin{aligned}
u_i^0 &= \frac{1}{2}(u_{i-1}+u_{i+1}) - \frac{c_1}{2E}(\sigma_{i-1}-\sigma_{i+1}) + \frac{\Delta x}{6}\{(D\sigma)_{i-1}-(D\sigma)_{i+1}\},\\
\sigma_i^0 &= -\frac{E}{2c_1}(u_{i-1}-u_{i+1}) + \frac{1}{2}(\sigma_{i-1}+\sigma_{i+1}) - \frac{E\Delta x}{6c_1}\{2(D\sigma)_i^0+(D\sigma)_{i-1}+(D\sigma)_{i+1}\},\\
v_i^0 &= \frac{1}{2}(v_l+v_r) - \frac{c_2}{2\mu}(\tau_l-\tau_r) + \frac{\Gamma}{2}\Delta x\{(D\tau)_l-(D\tau)_r\},\\
\tau_i^0 &= -\frac{\mu}{2c_2}(v_l-v_r) + \frac{1}{2}(\tau_l-\tau_r) - \frac{\mu\Gamma}{2c_2}\Delta x\{2(D\tau)_i^0+(D\tau)_l+(D\tau)_r\}.
\end{aligned} \tag{3.12}$$

The functions with suffixes l and r are expressed in terms of functions with suffixes i, $i-1$ and $i+1$, by means of the following second-order formulae:

$$\begin{aligned}
f_l+f_r &= 2f_l+\Gamma^2(f_{i-1}-2f_i+f_{i+1})+0(\Delta t^3),\\
f_l-f_r &= (f_{i-1}-f_{i+1})+0(\Delta t^3),
\end{aligned} \tag{3.13}$$

where $\Gamma = c_2/c_1$.

On the right-side of the Eqs. (3.12) appear the terms with superscript 0 containing unknown functions w_i^0. Therefore the iteration method is applied here, using as the first iteration the values of these functions with subscript i.

Before starting the numerical computations of our problem the initial and boundary conditions as well as material constants should be determined properly. By analogy with

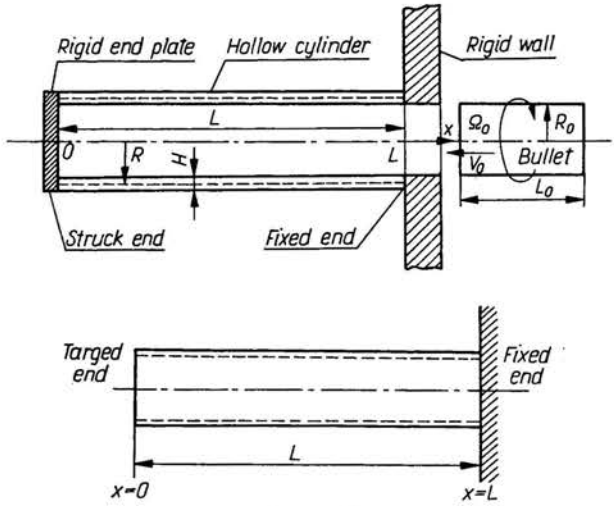

FIG. 3. The type of boundary-value problem for combined dynamic load.

the experiments performed in which the rotating bullet was striking a rigid target closing a hollow cylinder (specimen) which was fixed at the other end to the rigid wall, we named the corresponding boundary conditions as the "target" and "fixed end" conditions (Fig. 3). At the target end the velocities

$$u(0,t) = \tilde{u}(t), \quad v(0,t) = \tilde{v}(t), \tag{3.14}$$

the stresses

$$\sigma(0,t) = \tilde{\sigma}(t), \quad \tau(0,t) = \tilde{\tau}(t) \tag{3.15}$$

or mixed stress-velocity conditions may be prescribed. At the fixed end we have:

$$u(L,t) = v(L,t) = 0. \tag{3.16}$$

The initial conditions are prescribed for undisturbed case (for the region $t < x/c_1$)

$$u(x,0) = v(x,0) = \sigma(x,0) = \tau(x,0) = 0, \tag{3.17}$$

as well as for the prestressed conditions

$$u(x,0) = v(x,0) = 0, \quad \sigma(x,0) = \sigma_0^*, \quad \tau(x,0) = \tau_0^*. \tag{3.18}$$

To the evaluation of two remaining unknown functions at the target and the fixed end, the difference equations of the same order of accuracy should be derived. When the method of characteristics is applied it may easily be done by eliminating the difference equations along certain characteristics, i.e. for target points equations along the characteristics $(i-1, i^0)$ and (l, i^0), whereas for the fixed end points equations along the characteristics $(i+1, i^0)$ and (r, i^0), Fig. 2b. If the stress or velocity conditions are prescribed for target points, we obtain the following two sets of equations:

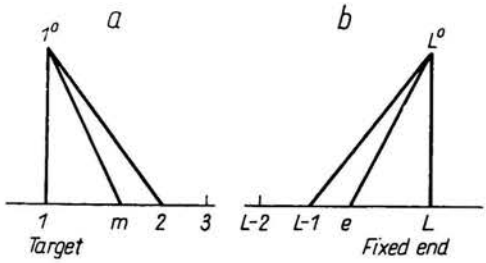

FIG. 4. a — Element of the characteristic net for target points. b — Element of the characteristic net for the fixed end points.

i) for stress conditions (Fig. 4a)

$$\begin{aligned} u_1^0 &= u_2 + \frac{c_1}{E}\sigma_2 - \frac{c_1}{E}\sigma_1^0 - \frac{\Delta x}{3}\{(D\sigma)_1^0 + (D\sigma)_2\}, \\ v_1^0 &= v_m + \frac{c_2}{\mu}\tau_m - \frac{c_2}{\mu}\tau_1^0 - \Gamma\Delta x\{(D\tau)_1^0 + (D\tau)_m\}, \end{aligned} \tag{3.19}$$

ii) for velocity conditions

$$\begin{aligned} \sigma_1^0 &= \frac{E}{c_1}u_2 + \sigma_2 - \frac{E}{c_1}u_1^0 - \frac{E}{3c_1}\Delta x\{(D\sigma)_1^0 + (D\sigma)_2\}, \\ \tau_1^0 &= \frac{\mu}{c_2}v_m + \tau_m - \frac{\mu}{c_2}v_1^0 - \frac{\mu}{c_2}\Delta x\{(D\tau)_1^0 + (D\tau)_2\}, \end{aligned} \tag{3.20}$$

where

$$f_m = \frac{(1-\Gamma)(2-\Gamma)}{2} f_1 + \Gamma(2-\Gamma) f_2 - \frac{(1-\Gamma)}{2} f_3.$$

For fixed end points we hawe (Fig. 4b)

$$u_L^0 = v_L^0 = 0,$$

$$\sigma_L^0 = \frac{E}{c_1} u_L - \frac{E}{c_1} u_{L-1} + \sigma_{L-1} - \frac{E}{3c_1} \Delta x \{(D\sigma)_L^0 + (D\sigma)_{L-1}\}, \tag{3.21}$$

$$\tau_L^0 = \frac{\mu}{c_2} v_L^0 - \frac{\mu}{c_2} v_e + \tau_e - \frac{\mu}{c_2} \Gamma \Delta x \{(D\tau)_L^0 + (D\tau)_e\},$$

where

$$f_e = \frac{(1-\Gamma)(2-\Gamma)}{2} f_L + (2-\Gamma) f_{L-1} - \frac{(1-\Gamma)}{2} f_{L-2}.$$

Since the mathematical investigation of the convergence and stability of approximate difference solution is difficult to perform, we have limited our consideration to the energy method. The energy balance equation may be obtained from the following relation

$$\int\int \mathbf{w} \cdot (\mathbf{A}\mathbf{w}_t + \mathbf{B}\mathbf{w}_x + \mathbf{C}) dx\, dt = 0 \tag{3.22}$$

which leads to

$$\int_0^L \left[\frac{\varrho}{2}(u^2+v^2)\right] dx + \int_0^L \left[\frac{\sigma^2}{2E} + \frac{\tau^2}{2\mu}\right] dx + \int_0^T \int_0^L \left[\frac{2}{3} D\sigma^2 + 2D\tau^2\right] dx\, dt \tag{3.23}$$

$$= -\int_0^T [u\sigma + v\tau]_{x=0} dt + \int_0^L \left[\frac{\varrho}{2}(u^{*2}+v^{*2})\right] dx + \int_0^L \left[\frac{\sigma^{*2}}{2E} + \frac{\tau^{*2}}{2\mu}\right] dx.$$

The integrals on the left-hand side of the Eq. (3.23) represent the kinetic, elastic and viscoplastic energy respectively, while the right-hand side terms are by turn the input energy, initial kinetic energy and initial elastic energy. The error of computation is determined by the formula

$$\text{Error} = 1 - \frac{E_{\text{def}} + E_{\text{kin}}}{E_{\text{inp}} + E_{\text{initial}}}, \tag{3.24}$$

where E_{def} denotes the deformation energy as a sum of elastic and viscoplastic energy, i.e.

$$E_{\text{def}} = E_{\text{elastic}} + E_{\text{viscoplastic}} = \int\int (u_x \sigma + v_x \tau) dx\, dt. \tag{3.25}$$

E_{kin} and E_{inp} are respectively the kinetic energy and input energy, whereas E_{initial} is a sum of initial kinetic and elastic energies.

4. Numerical results

For evaluation of the unknown functions u, v, σ, τ by means of the Eqs. (3.12)–(3.21), the computing programme was prepared in which different parameters as, for example,

loading functions, material constants, work-hardening, relaxation function or mesh size may easily be changed. Numerical computations were performed for mild steel and aluminium alloy. The following data were assumed in computations:

relaxation function: $(F) = \left(\frac{\sqrt{J_2}}{k} - 1\right)^p$

material constants:

(4.1)

for mild steel	for aluminium
$E = 2.1 \times 10^6\,\mathrm{kg/cm^2}$,	$E = 0.714 \times 10^6\,\mathrm{kg/cm^2}$,
$\mu = G = 0.82 \times 10^6\,\mathrm{kg/cm^2}$,	$G = 0.26 \times 10^6\,\mathrm{kg/cm^2}$,
$\sigma_0 = 4.2 \times 10^3\,\mathrm{kg/cm^2}$,	$\sigma_0 = 0.66 \times 10^3\,\mathrm{kg/cm^2}$,
$k = \tau_0 = 2.44 \times 10^3\,\mathrm{kg/cm^2}$,	$\tau_0 = 0.380 \times 10^3\,\mathrm{kg/cm^2}$,
$\gamma = 750\,\frac{1}{\mathrm{sec}}$,	$\gamma = 17.000\,\frac{1}{\mathrm{sec}}$,
$p = 1$,	$p = 4$,
$\varrho = 7.8 \times 10^{-6}\,\mathrm{kgcm^{-3}s^2}$,	$\varrho = 2.7 \times 10^{-6}\,\mathrm{kgcm^{-3}s^2}$.

Data (4.1) were determined on the basis of one-dimensional tests performed for mild steel by HARDING, WOOD and CAMPBELL [24] and for aluminium by KARNES and RIPPERGER [25]. The way of their evaluation is described in detail in [23].

Two loading functions at the target end are assumed:

i) "step" function, i.e. function increasing from zero to a certain value and then kept constant (Fig. 5). The increasing part of the curve should be very small and is introduced

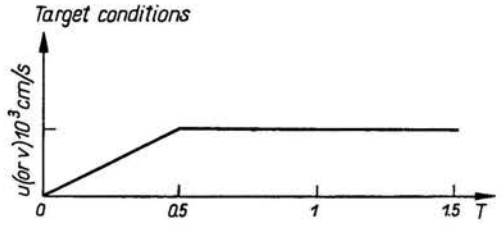

FIG. 5. "Step" load function.

here to avoid singularities in computation. T is dimensionless quantity and equals $c_1 t/L'$, $T = 1$ corresponds to the time necessary for longitudinal wave to reach the fixed end of a tube.

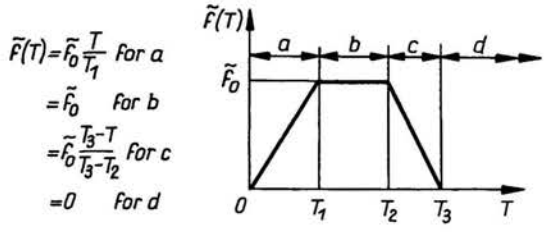

FIG. 6. "Impulse" load function.

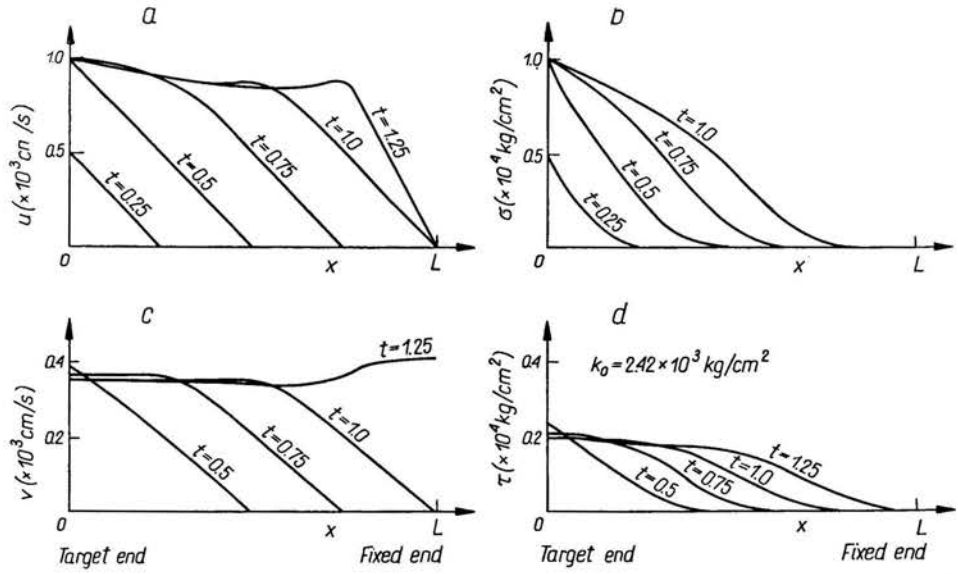

FIG. 7. a. Distribution of u along mild-steel tube for different times for "step" velocity target loading. b — Distribution of v along mild-steel tube for different times for "step" velocity target loading. c — Distribution of σ along mild-steel tube for different times for "step" velocity target loading. d — Distribution of τ along mild-steel tube for different times for "step" velocity target loading.

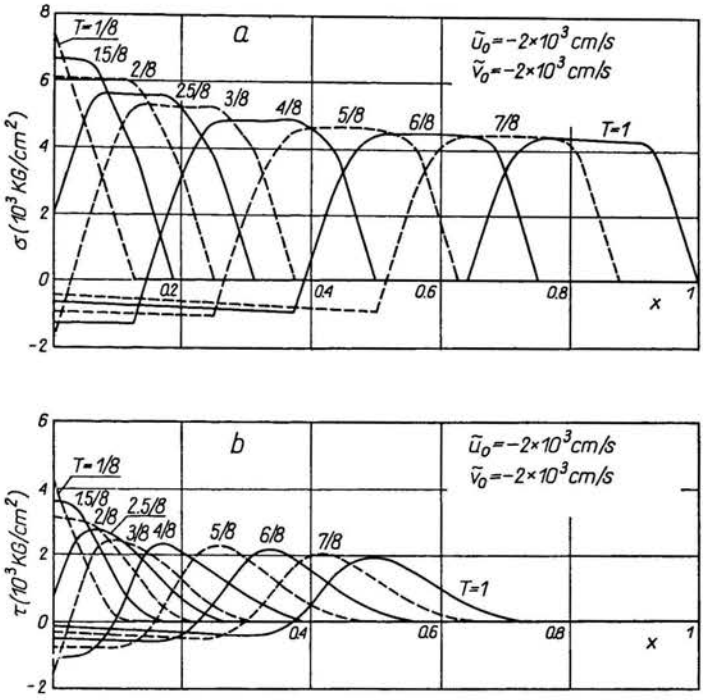

FIG. 8. a — Distribution of σ along mild-steel tube for different times for "impulse" velocity target loading. b — Distribution of τ along mild-steel tube for different times for "impulse" velocity target loading.

ii) impulse function (Fig. 6) $f(T)$ is described by the relation

$$\tilde{f}(T) = \begin{cases} \tilde{f}_0 \dfrac{T}{T_1}, & \text{for segment } a, \\ \tilde{f}_0, & \text{for segment } b, \\ \tilde{f}_0 \dfrac{T_3 - T}{T_3 - T_2}, & \text{for segment } c, \\ 0, & \text{for segment } d. \end{cases}$$

Such type of impulse is almost always observable in specimen during impact experiments.

The results of computations are presented in the form of diagrams. In Figs. 7a–7d typical curves of distribution of velocities u and v and the stresses σ and τ along a tube for different times in a case of "step" loading are given. The amplitude of load is sufficiently large to cause plastic deformations. It is seen from Figs. 7c and 7d that the diagrams of stresses σ and τ are linear in elastic range and the stresses propagate with elastic velocities c_1 and c_2, respectively. However, when the loading enters the plastic range, the velocities

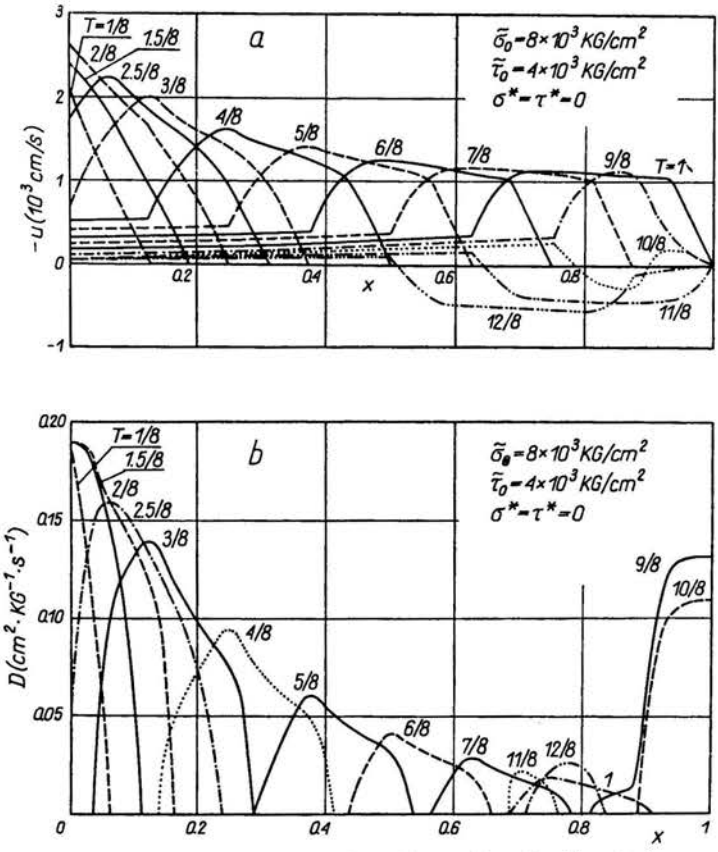

FIG. 9. a — Distribution of u along mild-steel tube for different times for "impulse" stress target loading. b — Distribution of the reduced relaxation function $D = \gamma\Phi(F)/\sqrt{J_2}$ for different times for "impulse" stress target loading.

of stress propagation decrease and the shape of the stress distribution changes gradually with increasing of time. The diagrams of v and τ in elastic region are not exactly linear, as are diagrams of u and σ, because they propagate in already disturbed region. Perhaps also the cumulated error of computation plays a certain role. An interesting phenomenon may be seen in Fig. 7a for the curve $T = 1$, where the positive gradient of the velocity u is observable. Since the explanation of this phenomenon is not possible immediately, we shall pay some attention to the problem of distribution of the stress gradients in our next work.

Let us analyze now the propagation of pulses caused by the load shown in Fig. 6. The numerical results for mild steel are presented in Figs. 8–10 and for aluminium in Figs. 11–12. Both zero and prestressed initial conditions are considered. Figures 8a and 8b show the variation of the stresses σ and τ along the tube for the case of the velocities prescribed at the target end. In Figs. 9a and 9b the distribution of the velocity u and the reduced relaxation function $D = \gamma F/\sqrt{J_2}$ is shown for stresses given at the target. The variations of shear stress ε and D along the tube for different times in a case of initially prestressed tube are presented in Figs. 10a and 10b, respectively. Distributions of the

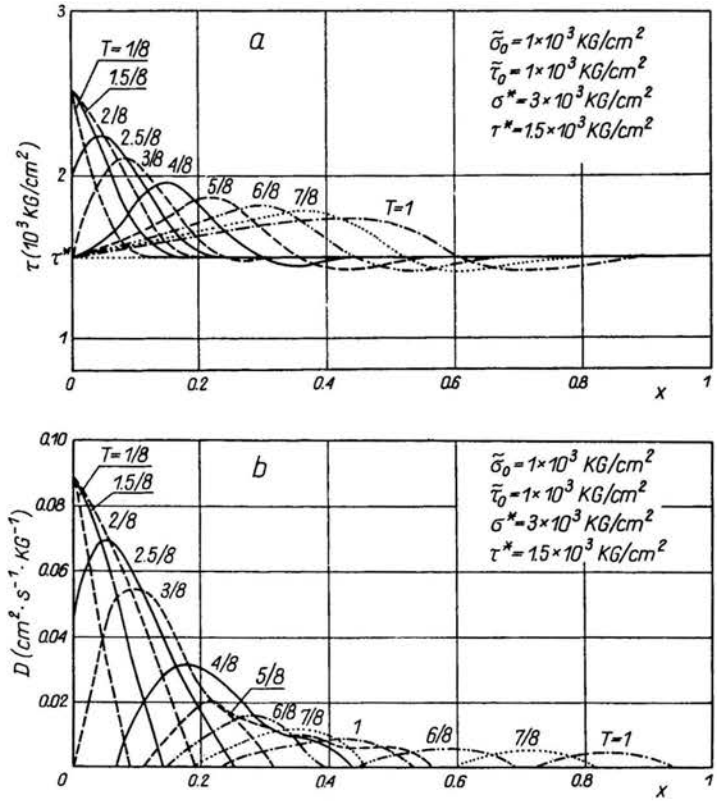

FIG. 10. a — Distribution of τ along prestressed mild-steel tube for different times for "impulse" incremental stress target loading. b — Distribution of D along prestressed mild-steel tube for different times for "impulse" incremental stress target loading.

a

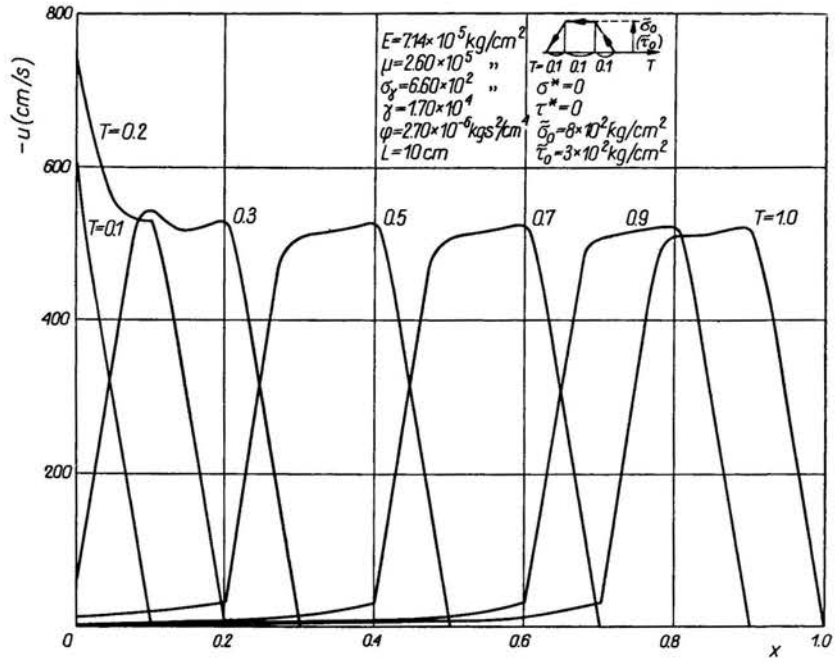

b

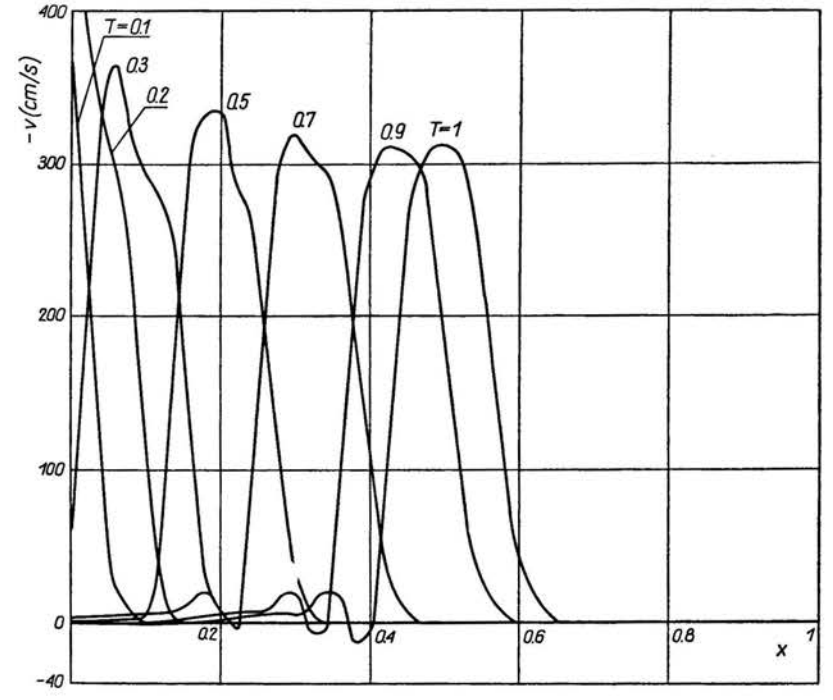

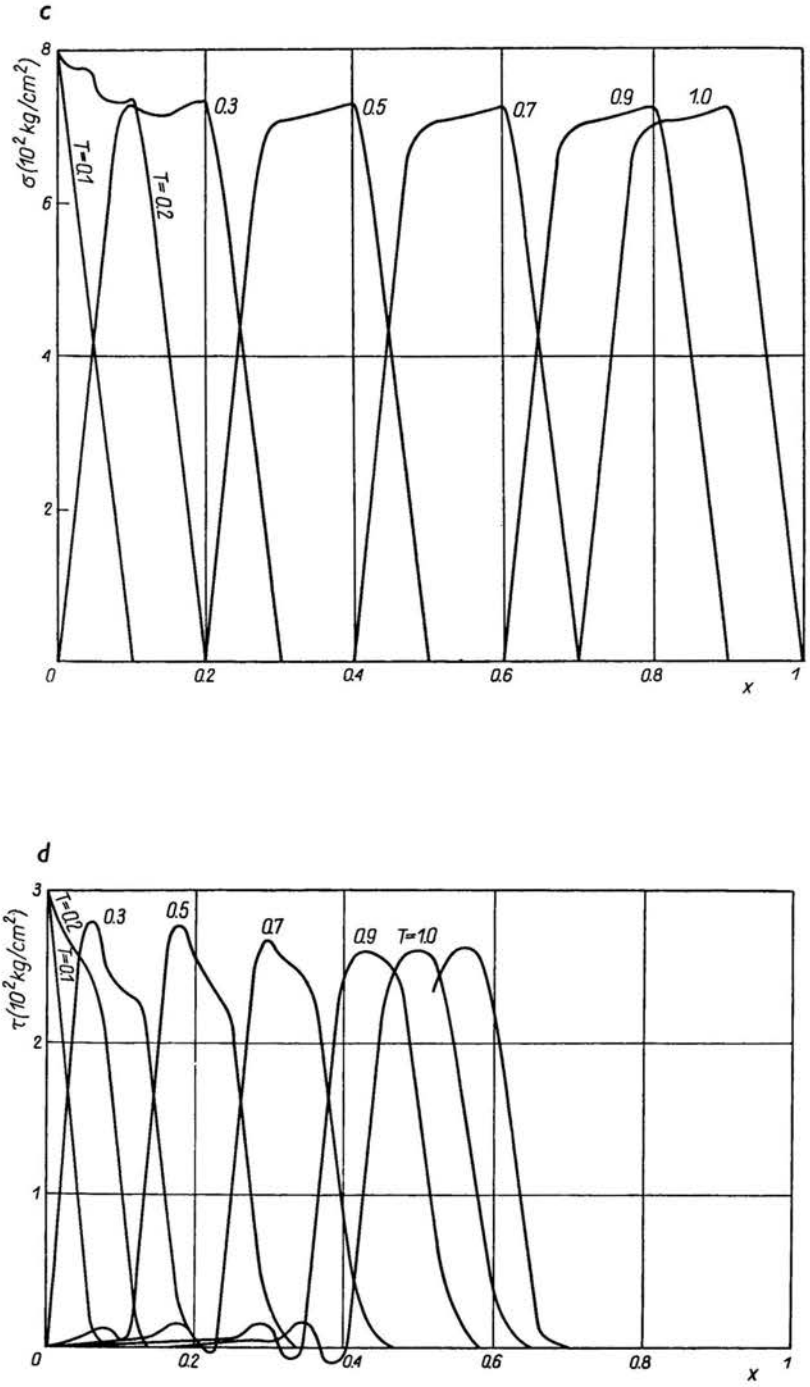

FIG. 11. a — Distribution of u along alumlnium tube for different times for "impulse" stress target loading. b — Distribution of v along aluminium tube for different times for "impulse" stress target loading. c — Distribution of σ along aluminium tube for different times for "impulse" stress target loading. d — Distribution of τ along aluminium tube for different times for "impulse" stress target loading.

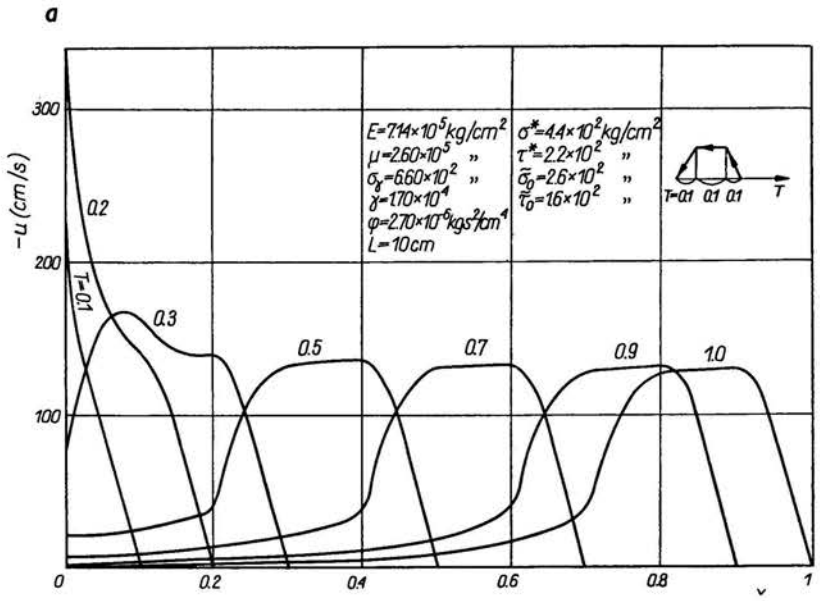

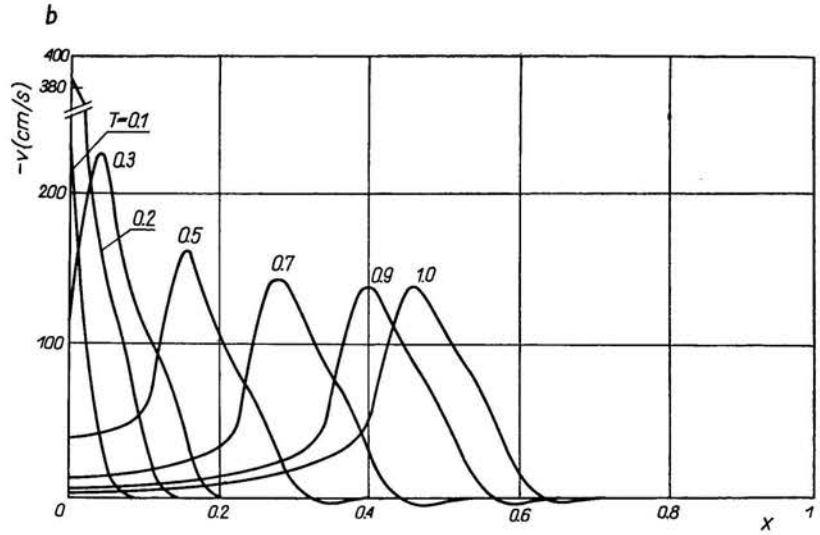

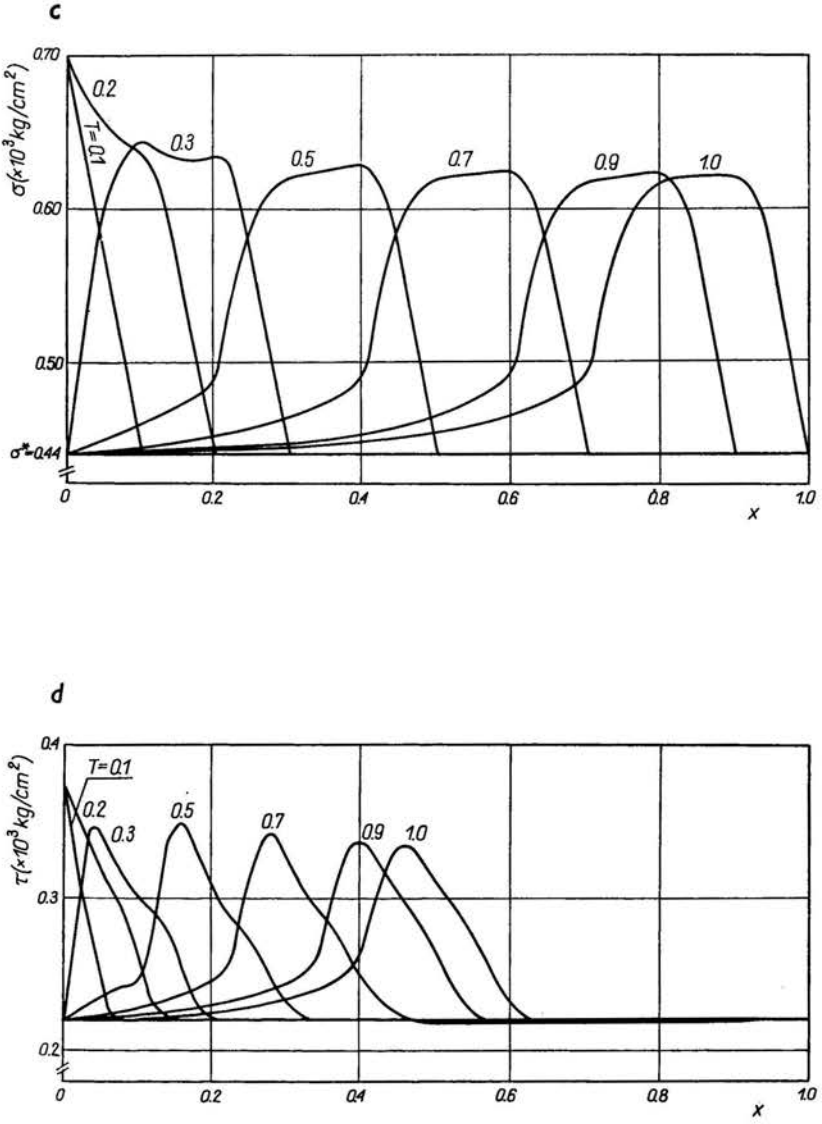

FIG. 12. a — Distribution of u along prestressed aluminium tube for different times for "impulse" incremental stress target loading. b — Distribution of v along prestressed aluminium tube for different times for "impulse" incremental stress target loading. c — Distribution of σ along prestressed aluminium tube for different times for "impulse" incremental stress target loading. d — Distribution of τ along prestressed aluminium tube for different times for "impulse" incremental stress target loading.

sought-for quantities u, v, σ and τ along the tube are demonstrated in Figs. 11a–11d for zero initial conditions and in Figs. 12a–12d for prestressed conditions.

From the figures presented some interesting wave phenomena in a combined state of stress in an elastic viscoplastic tube are observed. In general our results confirm the facts observed earlier experimentally and theoretically, but some of them, which will be mentioned below, seem to be new.

For a tube initially prestressed, the unloading wave propagates with the velocity ranging from the velocity of longitudinal wave to the velocity of shear wave (Fig. 10).

The boundary B dividing the elastic and viscoplastic region is propagating with the velocity of longitudinal wave c_1 (Fig. 8).

The value of relaxation function D decreases exponentially with time T (Fig. 9) and the attenuation is the quicker the larger is the value of initial loading, initial prestress or incremental loading. It is observed also that the attenuation of wave in aluminium tube is smaller than in mild steel tube.

In some situations two viscoplastic regions appear at the same time (Fig. 10).

In the case of velocity target conditions the negative values of stresses remain in the vicinity of the target after unloading (Fig. 8) and small values of velocity in the case of stress target conditions (Fig. 10).

During reflection of the longitudinal wave from the fixed end of a tube the region of large stresses suddenly appears and then rapidly decreases (Fig. 9b).

There are different shapes of a plane segment b of the pulse for aluminium and for mild steel (Fig. 8a and Fig. 11c). In the case of aluminium it is ascending, whereas for mild steel it is descending.

It was not possible to compare our results with experimental ones because up to now there are no confident and repetitive experimental data on combined stress wave propagation in a thin-walled tube made of mild steel.

Acknowledgement

The assistance of Mr H. TODA in numerical computations is greatly appreciated.

References

1. R. J. CLIFTON, *An analysis of combined longitudinal and torsional plastic waves in a thin-walled tube*, Proc. Fifth U.S. Nat. Congress Appl. Mech., 465–480, 1966.
2. H. FUKUOKA, *Infinitesimal plane waves in elastic plastic tubes under combined tension-torsion loads*, Proc. 16th Japan Nat. Congress Appl. Mech., Tokyo, 109–113, 1966.
3. J. LIPKIN and R. J. CLIFTON, *An experimental study of combined longitudinal and torsional plastic waves in a thin-walled tube*, Proc. 12th Int. Congress Appl. Mech., Eds. M. HETENYI and W. G. VINCENTI, Springer, 292–304, 1969.
4. H. FUKUOKA and T. MASUI, *Experiment on incremental impact loading of plastically prestressed aluminium*, 13th Japan Congress Mat. Res. Met. Mat., 106–109, March 1970.
5. H. FUKUOKA and T. MASUI, *Incremental impact loading of plastically prestressed aluminium by combined tension-torsion load*, Bull. ISME, 1974.

6. T. C. T. TING, *On the initial slope of elastic-plastic boundaries on combined longitudinal and torsional wave propagation*, J. Appl. Mech., **36**, 203–211, 1969.
7. T. C. T. TING, *A unified theory on elastic-plastic wave propagation of combined stress*, Proc. Symp. Foundations of Plasticity, Ed. A. SAWCZUK, Noordhoff International Publishing, Leiden, 301–316, 1973.
8. T. C. T. TING, *Plastic wave propagation in linearly work-hardening materials*, J. Appl. Mech., **40**, 4, 1045–1049, 1973.
9. R. P. GOEL and L. W. MALVERN, *Biaxial plastic simple waves with combined kinematic and isotropic work hardening*, J. Appl. Mech., **37**, 1100–1106, 1970.
10. S. KALISKI, W. K. NOWACKI and E. WŁODARCZYK, *The influence of strain hardening in the problem of propagation of plane loading and unloading biwaves in elastic-viscoplastic semi-infinite body*, Proc. Vibr. Probl., **8**, 4, 1967.
11. S. KALISKI, W. K. NOWACKI and E. WŁODARCZYK, *Plane biwaves in an elastic-viscoplastic semi-space*, Proc. Vibr. Probl., **8**, 2, 1967.
12. S. KALISKI, W. K. NOWACKI and E. WŁODARCZYK, *Propagation of plane loading and unloading biwaves in an elastic-viscoplastic semi-infinite body*, P. I. *Theory*, P. II. *Numerical analysis*, Proc. Vibr. Probl., **8**, 3, 1967.
13. W. K. NOWACKI, *Waves problems in a theory of plasticity* [in Polish], PWN, Warszawa 1974.
14. H. FUKUOKA, H. TODA, J. BEJDA, *Response of elastic viscoplastic thin-walled tube to the combined torsional and axial impact*, Materials Solid Mech. Conf., Hamamatsu, June 1974 (in Japanese).
15. P. PERZYNA, *Fundamental problems in viscoplasticity*, Adv. Appl. Mech., **9**, 1966.
16. J. C. C. HSU and R. J. CLIFTON, *Plastic waves in a rate sensitive material*. II. *Waves of combined stress*, J. Mech. Phys. Sol., **22**, 4, 255–266, 1974.
17. P. M. NAGHDI and S. A. MURCH, *On the mechanical behaviour of viscoelastic/plastic solids*, J. Appl. Mech., **30**, 321–328, 1963.
18. P. PERZYNA, *The constitutive equations for rate sensitive plastic materials*, Quart. Appl. Math., **20**, 321–332, 1963.
19. U. S. LINDHOLM, *Some experiments in dynamic plasticity under combined stress*, Symp. Mech. Behav. Mat. Dyn. Loads, Springer, 77–95, 1967.
20. U. S. LINDHOLM, *Dynamic deformations of metals*, in: "Behaviour of materials under dynamic loading", Am. Soc. Mech. Eng., 42–61, New York 1965.
21. P. PERZYNA, *Internal variable description of plasticity*, in: "Problems of plasticity", Ed. A. SAWCZUK, Noordhoff International Publishing, Leiden, 145–176, 1973. *Théorie physique de la viscoplasticité*, Bull. Acad. Polon. Sci., Série Sci. Techn., **21**, 123–139, 1973 and Centre Scientifique à Paris, Conferences, Fascicule 104, 1974.
22. R. COURANT and D. HILBERT, *Methods of mathematical physics*. II. Interscience Publ. N. Y., 1962.
23. P. PERZYNA and J. BEJDA, *The propagation of stress waves in a rate sensitive and work-hardening plastic medium*, AMS, **16**, 6, 1964.
24. J. HARDING, E. O. WOOD, J. D. CAMPBELL, *Tensile testing of materials at impact rates of strain*, J. Mech. Engrg. Sci., **2**, 88–96, 1960.
25. C. H. KARNES and E. A. RIPPERGER, J. Mech. Phys. Solids, **14**, 75, 1966.

POLISH ACADEMY OF SCIENCES
INSTITUTE OF FUNDAMENTAL TECHNOLOGICAL RESEARCH
and
OSAKA UNIVERSITY, FACULTY OF ENGINEERING SCIENCE
TOYONAKA, OSAKA, JAPAN.